ELSEVIER

Effect of gamma radiation on amlodis and its potential for radiosterilization

Mustafa Polat *, Mustafa Korkmaz

Physics Engineering Department, Hacettepe University, Beytepe, Ankara, Turkey

Abstract

In the present work, radiation sensitivity of amlodis (AML) and its active ingredient Amlodipin Besylate (AML-B) were separately investigated by electron spin resonance (ESR) spectroscopy using radiolytic products induced in these drugs. Irradiation in the dose range of 2.5–25 kGy did not create any ESR resonance line in AML-B, but it create five characteristic ESR resonance lines associated with more than one radical species in the case of AML. This signal is attributed to the radical species created upon irradiation of inactive ingredients such as microcrystalline cellulose and sodium starch glycolate of AML. Five resonance lines were observed to be divided into three sub groups of different characteristic behaviors associable with three different radical species. Radical species responsible from observed ESR lines were unstable at room and above room temperatures, however, they conserved their identities over a storage period of 92 days. This permitted to discriminate irradiated AML from unirradiated one. A quadratic function was found to describe best the variations of the intensities of observed resonance lines with applied radiation dose. A model based on three tentative radical species with a pyranose ring formed by the rapture of C−H bonds in positions 1 and 4 was proposed to explain the observed five lines experimental ESR spectra. AML was considered not providing the characteristic features of a good dosimetric material due to its low radiation yield and relatively fast decays of the created radical species, but very low radiation sensitivity of its active ingredient, namely AML-B makes AML a good candidate for radiosterilization.
© 2005 Elsevier B.V. All rights reserved.

Keywords: Amlodipin; ESR; Dosimetry; Temperature; Annealing

1. Introduction

Gamma radiation processing is a well-proven technique for achieving safe and effective sterilization of disposable medical devices and other medicinal products and also for improvement of the hygienic quality of foods [1–7]. Its major advantage is due to its high penetrating power and the very small temperature rise induced. The strong penetrating power of gamma radiation means that products can be sterilized after sealing into their final packaging, but the products are not heated and remain completely non-radioactive. The sterilization dose (Sterility Assurance Level (SAL) of 10^{-6}) of pharmaceuticals both depends on the initial microbiological spoilage and on the radio-sensitivity of the microorganisms [8]. On account of the destructive nature of ionising radiation and the difficulty in predicting the radiolytic effects, the study of radiation induced radicals and chemical products in drugs is necessary, both to determine the feasibility of the radiation treatment and to control it.

Detection and dosimetry of pharmaceuticals radiosterilization is a growing concern to numerous regulatory agencies worldwide; the ability to determine if a product has been irradiated may have a place in determining if a manufacturing method is being followed, or if there some doubt as to the veracity of a particular supplier. In this context, it is necessary to find methods of distinguishing between irradiated and non-irradiated pharmaceuticals. Electron spin resonance (ESR), which is a very sensitive method for detection of free radicals, can be used for detection of irradiated drugs [7,9–14] as already used elsewhere for foodstuffs irradiated [15–17].

The aims of the present work were: first, to investigate the radiation sensitivity of amlodis (AML) and its active ingredient Amlodipin Besylate (AML-B) in the dose range of 2.5–25 kGy; second, to develop mathematical functions to describe the dose–response curves of radiation induced ESR signals in irradiated AML; finally, to determine the dosimetric feature of AML from the kinetic behaviors of the radiation induced radical species over a large temperature range.

* Corresponding author. Tel.: +90 4 312 297 72 13; fax: +90 4 312 299 20 37.
E-mail address: polat@hacettepe.edu.tr (M. Polat).

2. Materials and methods

AML and its active ingredient AML-B were provided from Eczacıbaşı Pharmaceutical Company (Istanbul). AML-B ($C_{26}H_{31}ClN_2O_8S$) is a long-acting calcium channel blocker and its chemical name is 3-ethyl-5-methyl-2-(2-aminoethoxymethyl)-4-(2-chlorophenyl)-1,4-dihydro-6-methyl-3,5-pyridinedicarboxylate benzenesulphonate. AML-B is a white crystalline powder with a molecular weight of 567.1. AML is formulated as white tablets equivalent to 2.5, 5 and 10 mg of AML-B for oral administration. In addition to its active ingredient, each tablet contains the following inactive ingredients: microcrystalline cellulose, dibasic calcium phosphate anhydrous, sodium starch glycolate and magnesium stearate.

AML tablets were ground mechanically prior to irradiation and sieved through a No: 60 screen (0.25 apertures/mm) but AML-B is used as it was received, namely in its crystalline powder form. Samples are irradiated in polycarbonate vials. Ground AML tablets and AML-B in crystalline powder form were usually kept at room temperature (290 K) before irradiation treatment. All irradiation and ESR experiments were carried out on samples open to air in order to stay under commercial radiation sterilization conditions and to determine the possible dosimetric use of the studied AML and AML-B samples. Irradiations were performed at room temperature (290 K) using a ^{60}Co-γ source supplying a dose rate of 2.0 kGy/h in the sample position at the Sarayköy Nuclear Research Center of Turkish Atomic Energy Agency in Ankara. The dose rate was measured by Fricke dosimeter. A set of 21 samples irradiated to doses of 2.5, 5.0, 7.5, 10, 15, 20 and 25 kGy was employed to construct the dose–response curves. However, samples irradiated to a dose of 15 kGy were used to study the decay features of radiation-induced radicals at six different temperatures (313, 333, 353, 373 and 393 K). The former samples were kept at room temperature (290 K) before heat treatment.

ESR measurements were carried out using a Bruker EMX-131 X-band ESR spectrometer operating at 9.5 GHz and equipped with a high sensitive cylindrical cavity (conditions of operation: central field: 348.6 mT; scan range: 20 mT; microwave power: 0.5 mW; microwave frequency: 9.51 GHz; receiver gain: 2×10^4; modulation frequency: 100 kHz; modulation amplitude: 0.2 mT; time constant: 327.68 ms; sweep time: 83.886 s). Sample temperature inside the microwave cavity was monitored with a digital temperature control unit (Bruker ER 4111-VT). Each measurement corresponds to the average of at least three different samples. The position of the sample in the cavity was not changed during the long-term signal intensity decay experiment to avoid any error in g factor and intensity measurements arising from changes in the cavity-filling factor.

3. Experimental results and discussion

3.1. Unirradiated (control) and irradiated AML and AML-B samples

Unirradiated samples of mechanically ground AML and AML-B in crystalline powder form did not have any ESR signals.
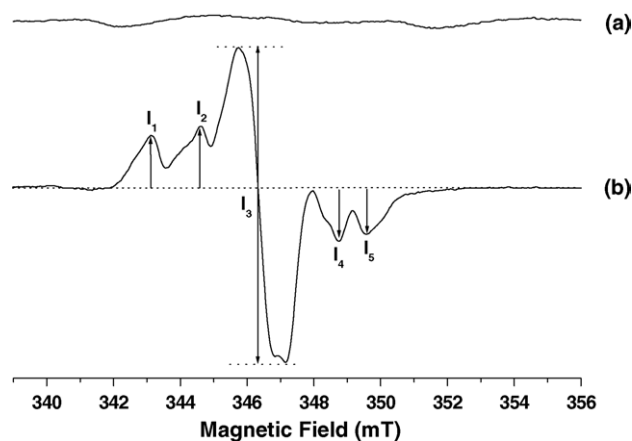

Fig. 1. ESR spectra of amlodis (AML). (a) Unirradiated (control) and (b) irradiated at 15 kGy.

However, while irradiated samples of AML exhibited an ESR spectrum with many lines, AML-B did not have any ESR signal in the irradiated dose range (2.5–25 kGy). Therefore, ESR measurements were performed on AML only. The ESR spectrum of AML was found to consist of a very intense central line at $g = 2.0033$ and four other resonance lines of doublet appearance positioned symmetrically at the both sides of the central line (Fig. 1). The shoulder observed on the negative lobe of the central line was considered as a sign of an axially symmetric radical species being responsible from this line. Studies carried out in the present work were based on the variations of the resonance peak intensities denoted as I_1, I_2, I_3, I_4 and I_5 (Fig. 1) under different experimental conditions. Variations of the peak intensities with microwave power were studied first, in the range of 0.1–20 mW. The results are given in Fig. 2. All measured intensities experienced continuous increases up to nearly 2.5 mW then they started to saturate. Above 2.5 mW, while other intensities experienced similar increases, I_3 was observed to experience
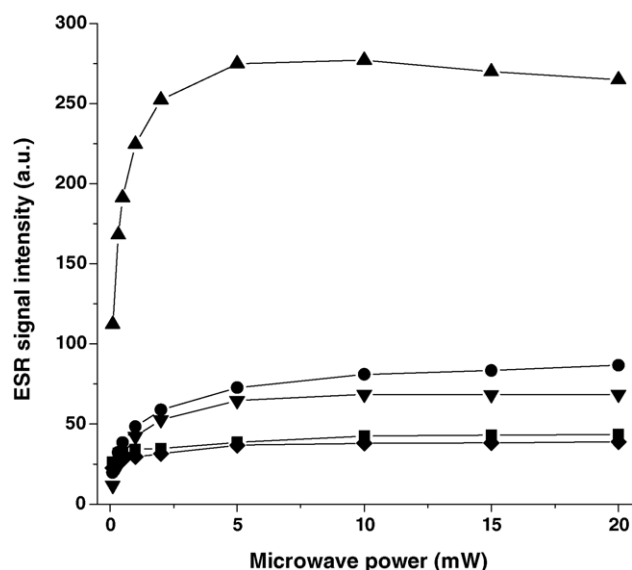

Fig. 2. Variations of the ESR peak intensities with applied microwave power; (■) I_1, (●) I_2, (▲) I_3, (▼) I_4, (♦) I_5.
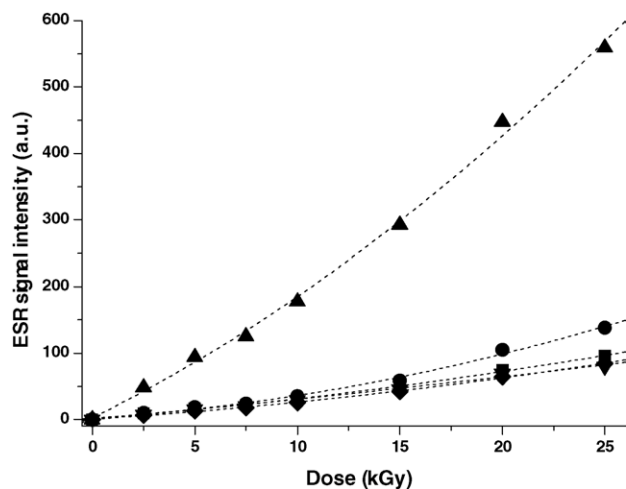
Fig. 3. Variations of the ESR peak intensities with absorbed radiation dose. (Symbols) experimental, (dashed) calculated; (■) I_1, (●) I_2, (▲) I_3, (▼) I_4, (♦) I_5.

a measurable decrease (Fig. 2). This difference in microwave saturation features of the signal intensities indicated clearly the existence of at least two radical species exhibiting different characteristics in irradiated AML. Basing on the results given in Fig. 2, 0.5 mW was adopted as microwave power in the rest of the work to avoid any saturation effect on measured intensities.

3.2. Dose–response curves

Samples of AML irradiated to doses of 2.5, 5.0, 7.5, 10, 15, 20 and 25 kGy were used to construct the dose–response curves through measured intensities. Variations of the measured intensities with absorbed radiation dose are given in Fig. 3. It is important to emphasize that pattern changes in the ESR spectrum were not observed in the studied dose range (2.5–25 kGy). The mathematical functions given in Table 1 were tried to describe

Table 1
Mathematical functions tried to describe dose–response data obtained for measured peak intensities

Function	Intensity	Parameters			r^2
		a	b	c	
$Y = a + bD$	I_1	−3.32	3.81	–	0.9944
	I_2	−9.83	5.51	–	0.9815
	I_3	−22.52	22.62	–	0.9944
	I_4	−1.49	3.30	–	0.9964
	I_5	−4.05	3.37	–	0.9931
$Y = a + bD + cD^2$	I_1	1.13	2.50	0.05	0.9981
	I_2	2.06	2.01	0.14	0.9943
	I_3	2.27	15.33	0.29	0.9971
	I_4	−0.20	2.92	0.01	0.9938
	I_5	0.55	2.02	0.05	0.9988
$Y = a + bD^c$	I_1	2.02	1.60	1.26	0.9973
	I_2	3.77	0.87	1.57	0.9934
	I_3	7.85	9.93	1.25	0.9970
	I_4	0.37	2.42	1.09	0.9941
	I_5	1.45	1.18	1.32	0.9982

the variations of the measured peak intensities with absorbed radiation dose without forcing them to pass from origin. In these functions, Y and D stand for the ESR peak intensity and absorbed radiation dose in kGy, respectively, and a, b and c are the constants to determine. As can be seen from Table 1, the biggest correlation coefficients are obtained in the case of quadratic and/or exponentially varying functions for measured intensities. However, the intercepts of the quadratic equation, which represent the intensities at zero applied radiation dose or the intensity of unirradiated sample, are smallest and, therefore, correlate well with the experimental results. Theoretical dose–response curves relevant to the measured peak intensities were also calculated using parameter values given in Table 1. They are also represented in Fig. 3 as dashed lines with their corresponding experimental counterparts. It is seen that agreement between experimental and theoretical data is fairly good and that the slope of the dose–response curve associated with I_3 intensity is bigger than the slopes of dose–response curves of the other intensities at all radiation doses. The peak intensities [I_1 (50 ± 4.0); I_2 (59 ± 5.0); I_3 (290 ± 20); I_4 (46 ± 4.0); I_5 (42 ± 3.0)] measured for a sample irradiated at a dose of 15 kGy were used together with a, b and c values given in Table 1 to calculate theoretical doses from quadratic equation. 14.8 ± 1.2; 14.3 ± 1.3; 14.7 ± 0.9; 14.7 ± 1.2; 14.8 ± 1.4 kGy dose values were calculated from I_1, I_2, I_3, I_4 and I_5 intensities given above, respectively. As is expected, error relevant to I_3 intensity is smaller compare with those obtained for other intensities. This means that, although not linear, a good accuracy in the dose determination can be achieved basing on a good calibrated dose–response curve of I_3 intensity.

3.3. Variable temperature studies

Variations with temperature of the peak intensities of an AML sample irradiated at a dose of 15 kGy were also investigated in the temperature range of 130–370 K. Variations of I_1, I_2, I_4 and I_5 intensities with temperature were similar over the temperature range, but that of I_3 intensity was different. This observation was considered again as an indication of the difference in nature of the radical species responsible from I_3 and other intensities (I_1, I_2, I_4, I_5). The results obtained for I_1 and I_3 intensities are given in Fig. 4a and b, respectively, as examples of these variations. The results concerning the other intensities are not given to save space. Cooling the sample from room temperature (290 K) down to 130 K produced practically no changes in I_3 intensity, however, it produced an increase in I_1 intensity. This is likely due to the saturation of I_3 intensity at low temperature even at the adopted microwave power (0.5 mW). When the sample was heated again from 130 K to room temperature, I_1 and I_3 intensities were observed to follow the same variation curves. Further heating of the sample produced irreversible decreases in I_1 and I_3. The decreases continued up to 370 K, which is the highest achievable temperature in the present experiment. Cooling the sample to room temperature from 370 K caused slight increases in both I_1 and I_3 intensities, but they never reached to their before heating values at 290 K. Although, heating created changes in the intensities, it did not produce significant changes
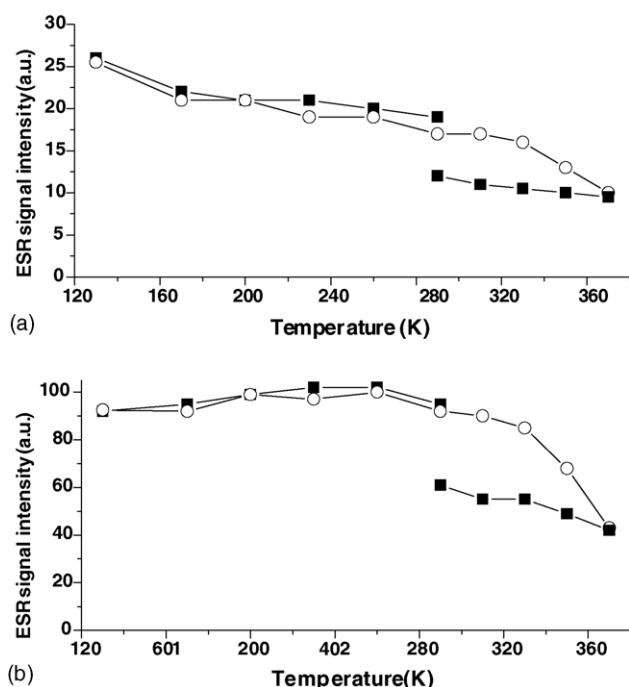
(a)

(b)

Fig. 4. Variation of the I_1 and I_3 intensities with temperature over a temperature range of 130–370 K; (a) I_1, (b) I_3. (■) Cooling; (○) heating.

in pattern and in other spectral parameters such as separation between peaks, g factors and line-widths.

3.4. Long-term stabilities of measured intensities at room temperature

Ground AML samples irradiated at 15 kGy were used to determine long-term room temperature stabilities of the studied intensities (I_1, I_2, I_3, I_4 and I_5). The samples were stored at room temperature (290 K) and their ESR spectra were recorded at regular time interval over a period of 92 days. I_3 intensity was found to decrease very fast in the first 30 storage days following the cessation of irradiation then this decrease became slower. Although having low radiation yields, I_1, I_2, I_4 and I_5 intensities were more stable than I_3. Time variations of the studied intensities at room temperature are given in Fig. 5. The following percent decreases of 59, 22, 62, 72, 60 were calculated to occur in I_1, I_2, I_3, I_4 and I_5 intensities, respectively, at the end of 92 days storage period without observable changes in the pattern and characteristic features of the ESR spectra.

3.5. Decreases in measured intensities at high temperatures

Studying the behaviors of the irreversible changes in the intensities above room temperature would be interesting from radical kinetics point of view. At high temperatures, irreversible decreases in intensities would be expected to originate from the decay of the magnetic units responsible for these intensities. The decay rates of these units at high temperatures should depend on the sample temperature. To test this idea and to get more insight into the decay processes of the radicals induced in irradiated AML, the samples were annealed at five different
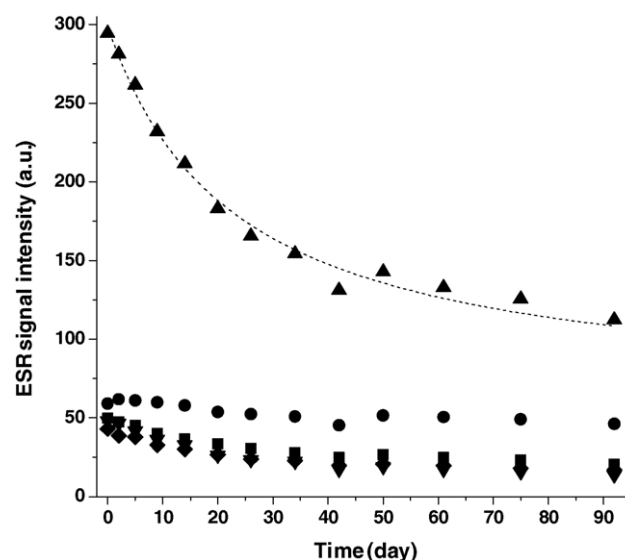

Fig. 5. Signal intensity decay curves at room temperature (290 K); (■) I_1, (●) I_2, (▲) I_3, (▼) I_4, (♦) I_5.

predetermined temperatures (313, 333, 353, 373 and 393 K) for predetermined times (3, 6, 10, 20, 40 and 60 min). Although, samples were annealed at high temperatures, all spectra were recorded at room temperature after cooling the samples to room temperature.

Analysis of microwave saturation, dose response, variable temperature and long-term signal intensity decay data revealed the presence of three groups of line intensities behaving differently, likely associated with three radical species of different spectroscopic features in gamma irradiated AML. Therefore, the activation energies of the radical species responsible from these groups of line intensities were calculated by annealing samples at high temperatures. Annealing was observed not creating changes in the pattern of ESR spectra except some decreases in the line intensities. These decreases in I_1, I_2, I_3, I_4 and I_5 intensities with annealing time at predetermined annealing temperatures were observed to follow second order kinetics. Thus, the decay constants (k) of the radical species associated with these intensities were calculated at each annealing temperature by fitting the experimental data to an expression (Eq. (1)) derived by integration of the differential equation describing second order kinetic behavior [18].

$$n = \frac{n_0}{n_0 kt + 1} \qquad (1)$$

where n_0 and n represents the signal intensities at zero and any time, t the annealing time and k is the decay constant. The decay constants calculated by this procedure are summarized in Table 2. Experimental and theoretical results derived from annealing studies for characteristic I_3 intensity are given in Fig. 6 as an example of the variations of studied intensities at the predetermined annealing temperatures. The results relative to the other intensities are not given to save space. As can be seen from Fig. 6, the agreement between experimental and calculated intensity variation results is fairly good.

Table 2
Calculated decay constants for radical species responsible from measured line intensities at five different annealing temperatures

Intensity	Annealing temperature (K)	Decay constant $k \times 10^4$ (h^{-1})	Activation energy (kJ/mol)
I_1	313	0.40	35.6 ± 0.5 ($r = 0.9997$)
	333	0.90	
	353	1.90	
	373	3.40	
	393	6.60	
I_2	313	8.60	56.8 ± 4.2 ($r = 0.9946$)
	333	42.40	
	353	127.90	
	373	280.10	
	393	–	
I_3	313	1.70	37.1 ± 1.3 ($r = 0.9981$)
	333	4.60	
	353	9.90	
	373	17.10	
	393	32.20	
I_4	313	0.10	38.5 ± 1.6 ($r = 0.9974$)
	333	0.30	
	353	0.60	
	373	1.20	
	393	2.10	
I_5	313	0.30	41.8 ± 1.2 ($r = 0.9988$)
	333	0.90	
	353	1.80	
	373	4.10	
	393	8.20	

The rate constant (k) is expected to exhibit an exponential dependence on temperature of the type $k = k_0 \, e^{-\frac{E_a}{RT}}$, where E_a is the reaction activation energy, R the gas constant and T is the absolute temperature [18]. If so, $\ln(k)$ versus $1/T$ plot should give a straight line whose slope is proportional to the reaction activation energy. The decay constants calculated from fitting at different annealing temperatures were used to con-
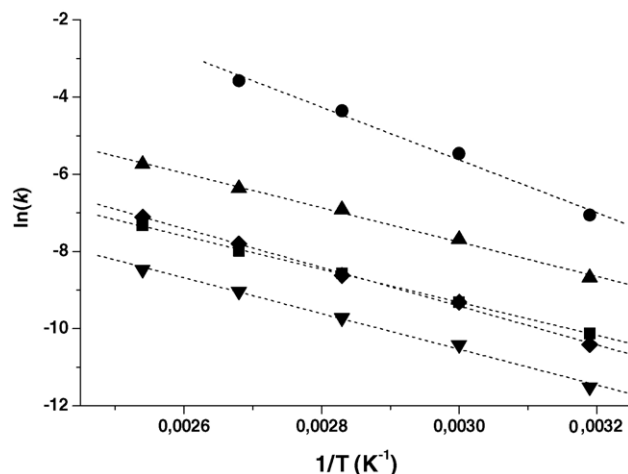
Fig. 7. Arrhenius plots constructed for radical species responsible from measured intensities of irradiated AML; (■) I_1, (●) I_2, (▲) I_3, (▼) I_4, (♦) I_5.

struct $\ln(k)$ versus $1/T$ plots. The results are summarized in Fig. 7. From the plot given in Fig. 7, the values of 35.6 ± 0.5, 56.8 ± 4.2, 37.1 ± 1.3, 38.5 ± 1.6 and 41.8 ± 1.2 kJ mol^{-1} K^{-1} were obtained for decay activation energies of the radical species responsible from I_1, I_2, I_3, I_4 and I_5 signal intensities, respectively. These results indicate that, the activation energy associated with I_2 line intensity (56.8 ± 4.2 kJ mol^{-1} K^{-1}) is fairly different from other energies whose magnitudes vary in a relatively short range (35.6–41.8 kJ mol^{-1} K^{-1}). This means that, at high temperatures, radical species responsible from I_2 line intensity decays very slowly compared with the other species responsible from I_1, I_3, I_4 and I_5 line intensities as they do at room temperature.

3.6. Spectra simulation

Simulation calculations were also performed using signal intensity data collected from room temperature spectra to characterize contributing radical species and to calculate their spectroscopic parameters. A model consisting of three radical species of different spectroscopic and decay features based on the analysis of the data derived from studies carried out in the framework of the present investigation was adopted throughout the calculations. The results of the calculations are summarized in Table 3. As is emphasized in Section 2, irradiation of AML-B, which is the active ingredient of AML, induces no radicals or radicals of very short lives not permitting to perform ESR measurement. Thus, observed ESR signal of irradiated AML would be expected to result from the degradation of un-medicinal ingredients of AML, especially from crystalline cellulose and sodium starch glycolate ingredients of this drug. Spectroscopic parameters calculated from spectrum simulation, which are given in Table 3, fall into the range of those observed for cellulosic radical species [19]. This result incited us to explore the possibility of creation of cellulosic radicals in irradiated AML and as a result of the exploration three tentative radical species given in Table 3 were proposed to explain experimental ESR spectra. The analysis of the calculated hyperfine splitting constants indicates
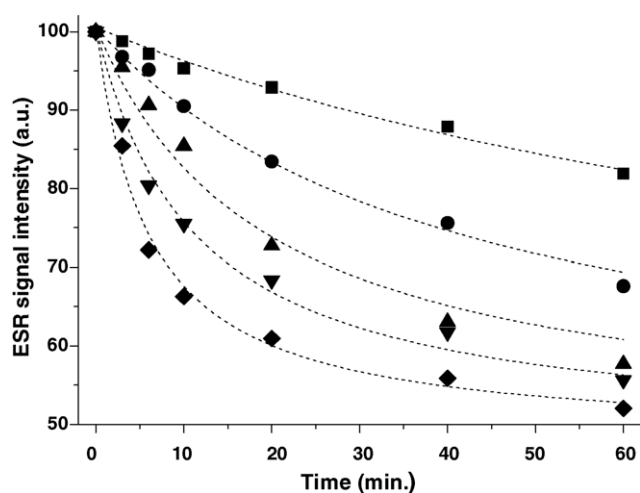

Fig. 6. Experimental and calculated decay curves for the radical species responsible from I_3 intensity at various annealing temperatures. Symbols—experimental: (■) 313 K, (●) 333 K, (▲) 353 K, (▼) 373 K, (♦) 393 K; solid lines (calculated).
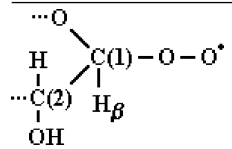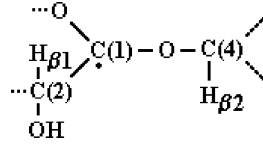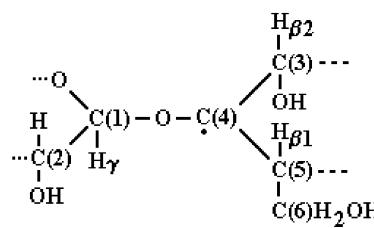
Table 3
Calculated ESR parameters for contributing radical species

Radical species	Percent weight	Proton	Hyperfine splitting (mT)			g factors			Line-width ΔH_{PP} (mT)
			A_x	A_y	A_z	g_x	g_y	g_z	
[structure: C(1)–O–O·, H, C(2) H$_\beta$, OH]	67.77	H$_\beta$	0.744	0.662	0.431	2.0101	2.0000	2.0024	0.314
[structure: C(1)–O–C(4), H$_{\beta1}$, C(2), OH, H$_{\beta2}$]	18.93	H$_{\beta1}$	3.242	2.327	3.180	1.9968	2.0023	2.0084	0.239
		H$_{\beta2}$	1.380	1.761	1.505				
		OH	0.577	0.374	0.223				
[structure: C(1)–O–C(4), with C(3), C(5), C(6)H$_2$OH ring, H$_{\beta2}$, H$_{\beta1}$, H$_\gamma$, OH]	13.30	H$_{\beta1}$	2.751	3.091	2.368	2.0031	2.0131	1.9977	0.233
		H$_{\beta2}$	2.035	0.178	1.524				
		H$_\gamma$	1.153	0.401	1.019				

that the ESR spectrum with many resonance lines may be due to the radicals with pyranose ring formed by the rapture of C−H bonds in positions 1 and 4. This agrees with the fact that the broken C−H bonds are in positions 1 and 4, which are weakened to great extent as a result of withdrawal of electron density at the 1, 4-β-glucoside bond and the ring oxygen atom [19].

Formation of a primary hydoxyalkyl (pHA) radical is a common event in crystalline carbohydrates containing a primary alcohol group when they are irradiated at low temperature [20]. Madden and Bernhard [21] reported that the main product was the C(6) hydoxyalkyl radical for α-D-glucopyranose irradiated at 77 K, while Dizdaroğlu et al. [22] found at room temperature that the free-radical population consisted mainly of C(1) and C(2) pHA and C(3) aldehydalkyl radicals. Theoretical spectrum calculated using parameters exposed in Table 3 and corresponding room temperature counterpart are given together in Fig. 8 for comparison. As seen the agreement between these spectra is relatively good. This indicates that the model based on three radical species summarized in Table 3 explains rather well the experimental ESR spectrum consisting of five resonance lines of gamma irradiated AML.

4. Conclusion

Unirradiated and irradiated AML-B (Amlodipin besylate) which is the active ingredient of amlodis (AML), was observed not exhibiting ESR signal. However, irradiated AML presented an ESR signal with five characteristic resonance lines originating from non-medicinal ingredients of this drug. Analysis of the experimental data derived from microwave saturation, dose response, variable temperature, long-term stability and annealing studies indicated that these characteristic lines designated as I_1, I_2, I_3, I_4 and I_5 can be divided into three sub groups associated with three different radical species and that a quadratic function describes best the variations of the intensities of these lines with applied radiation dose. Although, radical species responsible from observed line intensities were unstable at room temperatures, the shape of the ESR spectrum was observed to be conserved over a storage period of 92 days at room temperature. It was found that all line intensities could be detected and discrimination of unirradiated AML from irradiated one appeared to be possible even after a storage period of several months. However, AML does not present the characteristic features of a good dosimetric material for accurate dose measurements due to its low radiation yield and relatively fast decays of the observed resonance line intensities in spite of the presence of a radical species associated with I_2 line intensity having relatively high activation energy ($56.8 \pm 4.2\,kJ\,mol^{-1}\,K^{-1}$). A model based
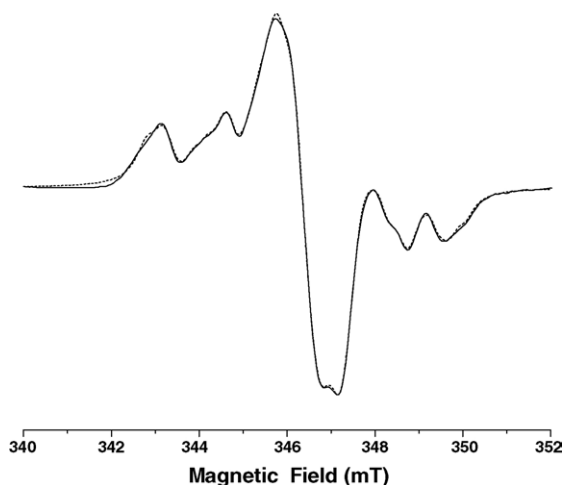

Fig. 8. Experimental and calculated ESR spectra for gamma irradiated AML; (—) experimental, (. . . . . .) theoretical.

on three tentative radical species proposed in the present work (Table 3) were found to describe fairly well the observed experimental spectra. Very low radiation sensitivity of AML-B was considered making AML a good candidate for radiosterilization.

Acknowledgement

References

[1] G.P. Jacobs, J. Biomater. Appl. 10 (1995) 59–96.
[2] B.D. Reid, PDA J. Pharm. Sci. Tech. 49 (1995) 83–89.
[3] B. Tilquin, B. Rollmann, J. Chim. Phys. PCB 93 (1996) 224–230.
[4] C. Boess, K.W. Bögl, Drug Dev. Ind. Pharm. 22 (1996) 495–529.
[5] L. Saint-Lebe, J. Raffi, Cah. Nutr. Diet. 30 (1995) 117–123.
[6] M. Polat, M. Korkmaz, Int. J. Pharm. 244 (2002) 169–179.
[7] M. Polat, M. Korkmaz, Int. J. Pharm. 255 (2003) 209–215.
[8] G.P. Jacobs, Rad. Phys. Chem. 26 (1985) 133–142.
[9] F. Zeegers, A.-S. Crucq, M. Gibella, B. Tilquin, J. Chim. Phys. PCB 90 (1993) 1029–1040.
[10] M. Gibella, A.-S. Crucq, B. Tilquin, J. Chim. Phys. PCB 90 (1993) 1041–1053.
[11] J.P. Basly, I. Longy, M. Bernard, Pharm. Res. 14 (1997) 1186–1191.
[12] J.P. Basly, I. Longy, M. Bernard, Pharma. Res. 14 (1997) 1192–1196.
[13] J.P. Basly, I. Longy, M. Bernard, Pharma. Res. 14 (1997) 810–814.
[14] J.P. Basly, I. Longy, M. Bernard, Anal. Chim. Acta 359 (1998) 107–113.
[15] J. Raffi, P. Stocker, Appl. Mag. Reson. 10 (1996) 357–373.
[16] M. Korkmaz, M. Polat, Rad. Phys. Chem. 58 (2000) 169–179.
[17] M. Korkmaz, M. Polat, Rad. Phys. Chem. 62 (2001) 411–421.
[18] W.L. Masterton, E.J. Slowinski, Chemical Principles, second ed., W.B. Saunders, Philadelphia, 1969, pp. 349–371.
[19] K.A. Dubey, P.K. Pujari, S.P. Ramnani, R.M. Kadam, S. Sabharwall, Rad. Phys. Chem. 69 (2004) 395–400.
[20] K.P. Madden, W.A. Bernhard, J. Chem. Phys. 84 (1980) 1712–1717.
[21] K.P. Madden, W.A. Bernhard, J. Chem. Phys. 86 (1982) 4033–4036.
[22] M. Dizdaroglu, D. Henneberg, K. Neuwald, G. Schomburg, C. Von Sonntag, Z. Naturforsch. B 32 (1977) 213–224.